Catalytic Liquid-Phase Nitrite Reduction: Kinetics and Catalyst Deactivation

Albin Pintar and Gorazd Berčič
Laboratory for Catalysis and Chemical Reaction Engineering, National Institute of Chemistry, Hajdrihova 19, SI-1001 Ljubljana, Slovenia

Janez Levec
Laboratory for Catalysis and Chemical Reaction Engineering, National Institute of Chemistry, Hajdrihova 19, SI-1001 Ljubljana, Slovenia
and
Dept. of Chemical Engineering, University of Ljubljana, Aškerčeva 5, SI-1001 Ljubljana, Slovenia

Liquid-phase reduction using a solid catalyst provides a potential technique for the removal of nitrites from waters. Activity and selectivity measurements were performed for a wide range of reactant concentrations and reaction conditions in an isothermal semi-batch slurry reactor, which was operated at temperatures below 298 K and atmospheric pressure. The effects of catalyst loading and initial nitrite concentration on the reaction rate were also investigated. The Pd monometallic catalysts were found to be advantageous over the Pd-Cu bimetallic catalyst with respect to either reaction activity or selectivity. Among the catalysts tested, minimum ammonia formation was observed for the Pd(1 wt. %)/γ-Al_2O_3 catalyst. The proposed intrinsic rate expression for nitrite disappearance over the most selective catalyst is based on the steady-state adsorption model of Hinshelwood, which accounts for a dissociative hydrogen adsorption step on the catalyst surface and an irreversible surface reaction step between adsorbed hydrogen species and nitrite ions in the Helmholtz layer. Both processes occur at comparable rates. An exponential decay in the activity of Pd(1 wt. %)/γ-Al_2O_3 catalyst has been observed during the liquid-phase nitrite reduction. This is attributed to the catalyst surface deprotonation, which occurs due to the partial neutralization of stoichiometrically produced hydroxide ions with carbon dioxide.

Introduction

Groundwater pollution by nitrates, which are perhaps the most ubiquitous of all groundwater contaminants, is a widespread problem in many locations in the world. Man-made or man-induced sources of nitrogen introduction into the subsurface environment include agricultural fertilizers, septic tank systems, and animal waste disposal. A number of hydrogeological factors and agricultural practices like precipitation/runoff, irrigation, soil type and depth, as well as geological features such as karst areas, denitrification, fertilizing intensity, crop types, and land usage influence the concentration of nitrates in groundwater at specific locations. Due to the incomplete abiotic and nitrification/denitrification processes in the soil, nitrite concentration in some groundwaters has been found at levels up to 3 mg/L (Vorlop et al., 1992). Since this value is significantly higher than the maximum contaminant concentration (that is, 0.02 mg/L) set by the European Drinking Water Directive, the nitrite content in such streams should be necessarily reduced in order to avoid health risk. The role of nitrite as a precursor to clinical cyanosis (blue baby syndrome) and carcinogenic nitrosamines, as well as to other N-nitroso compounds, is firmly established (Canter, 1996). Conventional physicochemical methods (such as reverse osmosis and electrodialysis), however, allow effective removal of nitrite ions from contaminated groundwater

Correspondence concerning this article should be addressed to A. Pintar.

by concentrating them in a secondary waste stream, which has called for new and environmental friendly systems. The most promising techniques for nitrite removal, without any occurrence of wastewater, are biological digestion (Kapoor and Viraraghavan, 1997) and catalytic denitrification (Vorlop and Tacke, 1989; Hörold et al., 1993a,b). Biological denitrification processes (either heterotrophic or autotrophic) are known to have great potential for the treatment of municipal and industrial wastewater streams. The main reasons for the slow transfer of technology to drinking water purification are concerns over possible bacterial contamination of treated water, the presence of residual organics in treated water, and the possible increase in chlorine demand of purified water. The reduction of aqueous nitrite solutions by using hydrogen over a solid catalyst offers an alternative and economically advantageous process to biological treatment as a means of purifying drinking water streams. This process can be represented by the following overall reaction

$$2NO_2^- + 3H_2 \xrightarrow{Pd/\gamma - Al_2O_3} N_2 + 2OH^- + 2H_2O \qquad (1)$$

Nitrites are selectively converted to nitrogen in a two- or three-phase reactor operating at mild reaction conditions (such as $T = 278-298$ K; $p(H_2) \leq 1$ bar). To maintain electroneutrality of the aqueous phase, consumed nitrites are replaced by hydroxide ions. The main drawback of this method is formation of the side product ammonia, which is undesirable in drinking water. Since catalytic liquid-phase hydrogenation of aqueous nitrite solutions is in a stage of development, it is obvious that more kinetic and mechanistic studies in aqueous solutions are needed in order to develop an effective catalytic process for purifying drinking water streams and industrial effluents.

Relatively few investigations have been published on the reduction of nitrites in aqueous solutions. It is reported by Hörold et al. (1993a,b) that among numerous noble metals (such as Pd, Pt, Ru, Ir, Rh) capable of promoting nitrite reduction, only the supported Pd catalysts represent satisfactory performance. In order to prepare a more selective catalyst, these authors varied the Pd-precursor for the impregnation, the Pd-loading (from 0.1 to 5 wt. %), and the support (aluminas and silicas). When Pd catalysts were prepared by the impregnation of macroporous silica supports with aqueous solutions of $Pd(NH_3)_4(OH)_2$, lower nitrite removal activities, with much higher selectivities, were obtained. The lowest formation of ammonia (selectivity of 99.9%) was observed with 0.8 wt. % of palladium on the silica support with an average pore diameter of 50 nm and BET surface area of 80 m^2/g. In this way, it was possible to reduce 100 mg/L of nitrite without exceeding the European Community permitted level of ammonia in drinking water (that is, 0.5 mg/L). Vorlop and Tacke (1989) and Hörold et al. (1993a) found that the nitrite removal activity, as well as the formation of ammonia, strongly depend on the pH value of the aqueous solution; with respect to higher nitrite disappearance rate, it is advantageous to carry out the reaction at low pH values. Furthermore, Vorlop et al. (1992) and Strukul et al. (1996) report that by using catalysts with larger particles (diameter above 0.5 mm) lower reaction selectivity is observed, which is due to the enhanced ammonia production. Pintar and Kajiuchi (1995) have found out that lower reaction selectivity might be attributed to the slow counter-diffusion of formed hydroxide ions from catalyst pores into the bulk liquid phase.

Quantitative rate data concerning the catalytic liquid-phase nitrite reduction are scarce. Tacke and Vorlop (1993) determined the kinetics of liquid-phase nitrite hydrogenation over a Pd/γ-Al_2O_3 catalyst containing 5 wt. % of Pd. The measurements were performed in a slurry reactor at $T = 276-297$ K. The initial rate kinetic data were analyzed by means of the differential method resulting in the rate expression of power-law type. They found the reaction rate to be of order 0.6 with respect to nitrite and independent of hydrogen partial pressure provided that this pressure is greater than about 1.0 bar. It is further reported that the observed rate per unit weight of the catalyst is not affected by the catalyst concentration. The apparent activation energy was found to be 31 kJ/mol. Nevertheless, the rate equation proposed by Tacke and Vorlop (1993) is useless when catalytic liquid-phase nitrite reduction is carried out at hydrogen partial pressures lower than 1 bar.

Pd-Cu/γ-Al_2O_3 solids are known as powerful catalysts for liquid-phase nitrate reduction (Hörold et al., 1993a,b; Pintar et al., 1996); however, the capability of Pd-Cu bimetallics synthesized by means of a multistep wet-impregnation technique to catalyze reductive nitrite destruction has not been investigated yet. Therefore, the objectives of this work are: (1) to evaluate the potential of Pd monometallic and Pd/Cu bimetallic catalysts for active and selective transformation of nitrites to nitrogen in the presence of either distilled or tap water as the reaction medium; and (2) to present a detailed kinetic study of catalytic liquid-phase hydrogenation of aqueous nitrite solutions aimed at the development of a rate equation for the design and modeling of a large-scale reduction reactor. Reaction rate and selectivity data were collected in an isothermal semi-batch slurry reactor. The values of kinetic parameters, included in different rate equations, typical of heterogeneous catalytic systems, were derived by means of the integral kinetic analysis. The results obtained are discussed in terms of the processes that take place at the catalyst-electrolyte interface. Finally, the chemical stability of the catalysts employed was examined.

Experimental Studies

Catalyst preparation

The liquid-phase reduction of aqueous nitrite solutions by hydrogen was studied using two monometallic Pd/γ-Al_2O_3 catalysts (labeled as CAT-1 and CAT-2) with different palladium loadings (1 and 5 wt. %), and a Pd-Cu/γ-Al_2O_3 bimetallic catalyst (designated as CAT-3). The solids were synthesized by a multistep wet-impregnation of the powdered alumina support (γ-Al_2O_3 of high purity from Nikki-Universal; NST-3H type; pore diameter: 10–25 nm) with an acidified aqueous solution of $PdCl_2$ (p.a., Fluka) in the case of CAT-1 catalyst, or with aqueous solutions of palladium and copper nitrate in the case of CAT-2 and CAT-3 catalysts. After every alumina impregnation step, the resulting solids were dried at 423 K. The catalyst preparation procedures were carried out as follows:

Table 1. Properties of Support and Hydrogenation Catalysts

Material	Metal Loading, wt. %	S_{BET}, m^2/g	iep, /
γ-Al_2O_3 support	—	154	8.5
CAT-1	1% Pd	149	6.4
CAT-2	5% Pd	146	8.6
CAT-3	4.7% Pd, 1.4% Cu	142	8.8

CAT-1: impregnation by an HCl acidified aqueous solution of $PdCl_2$, drying, and reduction (2 h, 773 K in H_2);

CAT-2: impregnation by palladium nitrate, drying, calcination (3 h, 773 K in air), and reduction (1 h, 773 K in hydrogen atmosphere);

CAT-3: impregnation by copper nitrate, drying, calcination (1 h, 773 K in air), impregnation by palladium nitrate, drying, calcination (3 h, 773 K in air), and reduction (1 h, 773 K in H_2).

The concentrations of metallic palladium and copper phases (ICP-AES analysis), the surface area (BET method), and the isoelectric point (iep) of catalysts are given in Table 1. The zeta potential of catalyst suspensions (0.07 wt. % in distilled water) was measured by means of a laser zee meter (Pen Chem, model 501) at $T = 293$ K and different pH values, which were adjusted by adding 0.1 M HCl or 0.1 M NaOH solutions. The resulting zeta potential vs. pH dependencies for the alumina support and various catalysts are represented in Figure 1a. It is seen that there is a downshift in the iep of the CAT-1 catalyst, which is a direct consequence of the preparation procedure. It is well known that Cl^- is strongly bound to γ-Al_2O_3, and its presence might lower the iep of the support even at low concentrations. By means of bulk chemical analysis, the concentration of chloride in fresh CAT-1 sample was found to be 0.3 wt. %. Furthermore, the dependencies presented in Figure 1a exhibit maxima at a pH value of aqueous solution close to 4, which is associated with the instability of alumina support in acidic aqueous solutions (Ponec and Bond, 1995). The prepared solids have X-ray powder diffraction patterns similar to the one of γ-Al_2O_3 support (Figure 1b). No peaks assigned to palladium- or copper-containing phases were detected, which suggests the presence of highly dispersed metallic phases; this was also confirmed by EDAX and EXAFS examination (Batista et al., 1997; Pintar et al., 1998a). A detailed comparison of X-ray diffractograms of the alumina support and synthesized solids shows that the catalyst preparation procedure mainly influences the peak position at 2Θ close to 40° (Figure 1b), which can be attributed to the preferred diffusion of Cu and Pd atoms into the γ-Al_2O_3 lattice (Strohmeier et al., 1985; Strukul et al., 1996).

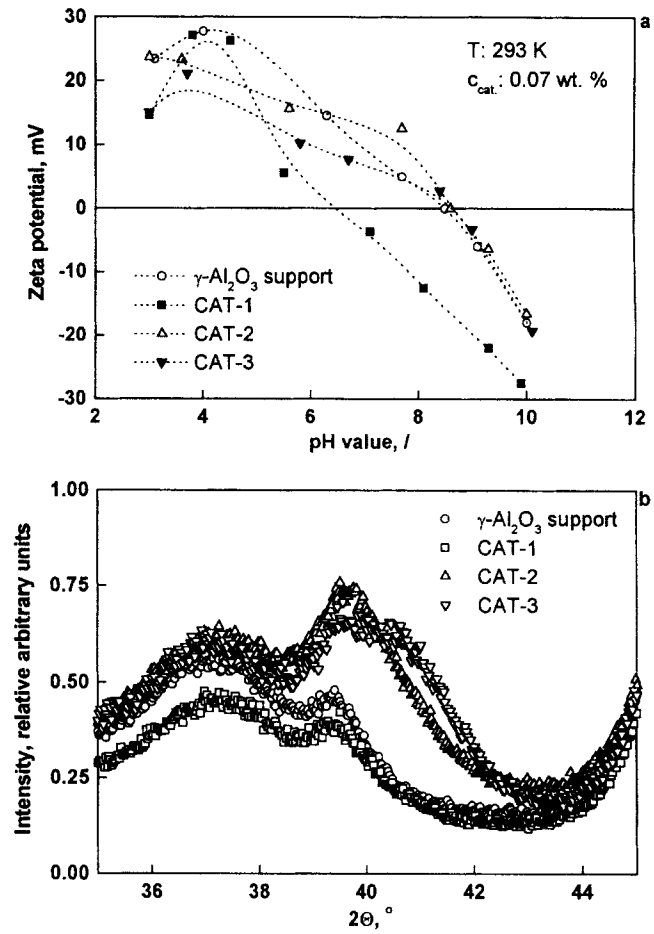

Figure 1. Zeta potential as a function of pH value (a) and X-ray diffractograms (b) of various monometallic and bimetallic catalysts tested in this study.

Apparatus and experimental procedure

Measurements were carried out in a 2.0-L reactor made of Pyrex glass, and equipped with a stirrer and a temperature control unit. Since the liquid-phase nitrite reduction can also be promoted by physical mixtures consisting of supported hydrogenation catalysts and metallic particles (Pintar and Kajiuchi, 1995; Batista et al., 1997), the reactor was free of metal parts in order to eliminate their effects on the measured nitrite conversions. The temperature of the reaction mixture was successfully controlled within ± 0.1 K of the set value by employing a PID control. No temperature rise due to the heat of reaction was observed in any of the runs, because the reactor was operated with low nitrite concentrations (up to 30 mg/L). No pressure control was required since the total operating pressure was equal to atmospheric pressure. The hydrogen and carbon dioxide flows, introduced into the vessel below the impeller, were controlled by electronic mass-flow controllers. Three phases were present in the reactor, so the entire system is treated as a slurry reactor.

The range of experimental conditions used in this work is listed in Table 2. In a typical run, a given amount of fresh (and previously reduced) catalyst was charged into the reactor containing 1.4 L of distilled water. The content of the reactor was purged with nitrogen, and then continuously sparged at a metered rate with a gas mixture of hydrogen and carbon dioxide, the latter being used as a hydrogen diluting agent. When the temperature of the reactor system was constant and equal to the set value, a concentrated solution (100 mL) of nitrites, prepared from reagent-grade $NaNO_2$, was introduced into the slurry. The pH value of the aqueous phase was kept constant during the reaction course at a value of 4.7 ± 0.1 by means of CO_2, according to the reactions

Table 2. Range of Reaction and Operating Conditions of the Catalytic Liquid-Phase Nitrite Hydrogenation Carried Out in Slurry Reactor

Reaction temperature, K	283–298
Hydrogen partial pressure, bar	0.11–1.0
Total operating pressure, bar	1.0
Catalyst concentration, mg/L	15–150
Average catalyst particle diameter, μm	25
Initial nitrite concentration, mg/L	5.0–30.0
Stirrer speed, rpm	400–600
Gas flow rate, mL_n/min	300–600
Reaction volume, L	1.5

$$2OH^- + CO_2 \rightarrow CO_3^{2-} + H_2O \quad (2)$$

$$CO_3^{2-} + CO_2 + H_2O \rightarrow 2HCO_3^- \quad (3)$$

To monitor the progress of the reaction under consideration, representative samples were withdrawn periodically (the time period was a function of experimental conditions) and the catalyst was immediately separated from the aqueous phase by centrifugation. The aqueous phase was then analyzed for the residual content of nitrites, as well as instantaneous concentration of ammonium ions.

External mass-transfer resistance can be dependent on the stirrer speed. Runs were conducted for various stirrer speeds and for different H_2-CO_2 flow rates with the resulting nitrite disappearance rates independent of both these variables in the range investigated (Table 2). In the additional blank runs (that is, absence of catalyst or hydrogen), no nitrite conversion was observed.

Analysis

The concentrations of nitrite ions in the aqueous-phase samples were determined by employing a UV/VIS spectrophotometer (Perkin-Elmer, model Lambda 40P) combined with the X-Y autosampler and flow-injection analyzer (Perkin-Elmer, model FIAS 300). A flow cell with a volume of 18 μL and optical pathlength of 10 mm was installed in the sample compartment of the UV/VIS spectrophotometer, thus enabling instantaneous response. The nitrite ion analysis was carried out in the VIS-range at $\lambda = 540$ nm using the naphthylamine analytical procedure. Distilled water was used as the mobile phase, and the flow rate of the latter was set to 280 mL/h in order to ensure linear system response in the concentration range 0–40 mg/L of nitrites. The flow of the mobile phase and reagents through the tubing and loops was arranged in such a way that a sample was injected according to the branched FIA technique. For the described analytical method, the relative analysis error was found to be below 0.5%. To evaluate concentrations of ammonium ions formed during the catalytic liquid-phase nitrite reduction, the gas-diffusion/acid-base indicator analytical procedure was applied using the same apparatus. In order to check for any evolution of hydroxylamine during the catalytic nitrite reduction, aqueous-phase samples were further analyzed following the procedure proposed by Johnson (1968). The pH values of the samples were determined by employing a digital pH meter (Orion, model 710A) equipped with a Ross combination electrode and ATC probe.

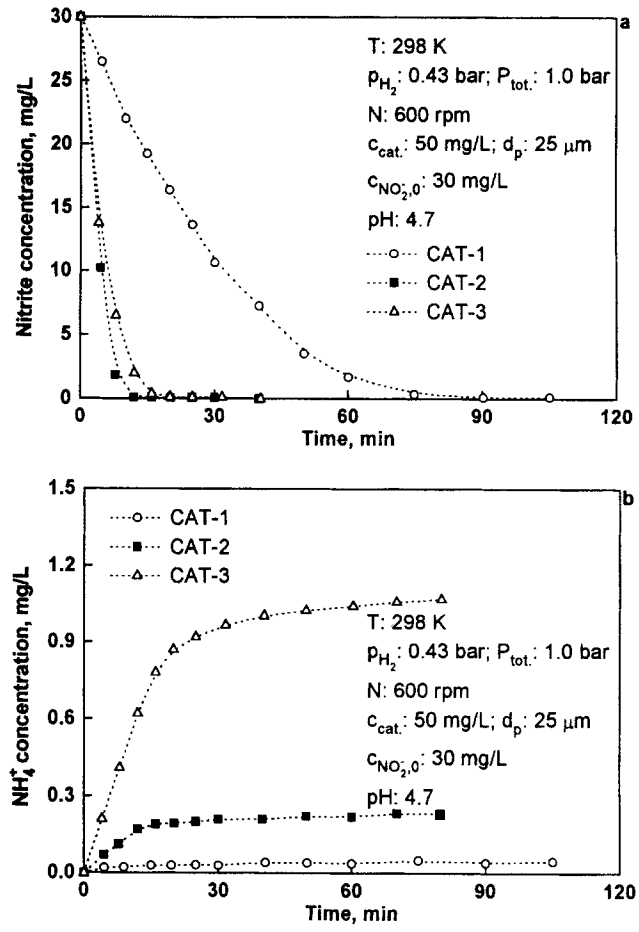

Figure 2. Nitrite (a) and ammonium (b) ions concentration vs. time dependencies obtained in the slurry reactor over various monometallic and bimetallic catalysts.

Results and Discussion

Typical concentration vs. time dependencies for nitrite and ammonium ions obtained during the catalytic liquid-phase nitrite reduction in the slurry reactor at a constant pH value of 4.7 are illustrated in Figure 2. It can be seen from Figure 2a that at the employed reaction conditions, the Pd(5 wt. %)/γ-Al_2O_3 catalyst exhibits the highest activity for nitrite removal, while the activity of the alumina-supported Pd(1 wt. %) sample is correspondingly lower. Although Pd-Cu bimetallics are effective catalysts for liquid-phase nitrate reduction (Hörold et al., 1993a,b), the resulting curve for the CAT-3 sample demonstrates that addition of copper to the Pd metallic phase has no beneficial effect on the measured nitrite conversions. Based on this experimental fact and the results of EXAFS investigation (Pintar et al., 1998a), which show that Pd and Cu form a substitutional solid solution, one can conclude that the role of copper is primarily that of an inert diluent exerting a geometric effect by breaking up ensembles of palladium atoms which constitute active sites for nitrite hydrogenation. Similar observations are reported also by other investigators (Skoda et al., 1994; Pintar and Kajiuchi, 1995). Furthermore, a comparison of the data with those

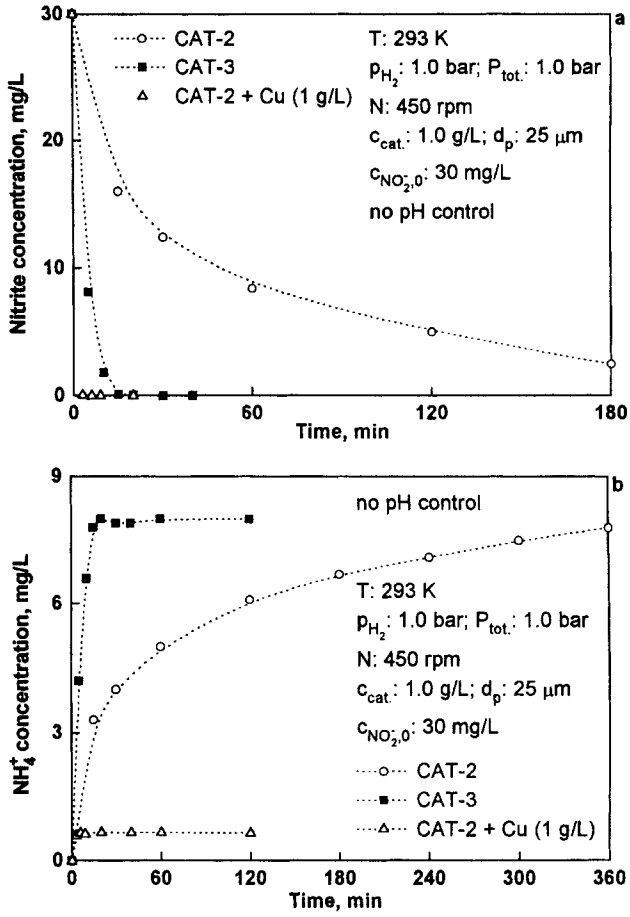

Figure 3. Nitrite (a) and ammonium (b) ions concentration-time profiles obtained in the course of liquid-phase nitrite hydrogenation over different catalytic systems.

of the catalytic liquid-phase nitrate reduction (Pintar et al., 1996; Batista et al., 1997) shows that, at the same reaction conditions, nitrite disappearance rates are greater by about one order of magnitude. As demonstrated in Figure 2b, minimum production of ammonium ions was observed in the presence of the CAT-1 sample. In this case, the reaction selectivity (at complete nitrite transformation) was equal to 99.5 mol. %. When the liquid-phase nitrite reduction was carried out over the supported Pd catalyst with a higher metal loading (CAT-2), the formation of ammonia was five times higher. On the other hand, Figure 2b illustrates that the production of ammonium ions is particularly enhanced by the deposition of the copper metallic phase on the alumina support.

The experiments illustrated in Figure 2 were carried out at a constant pH value of the aqueous solution; the hydroxide ions desorbed from the catalyst surface were, accordingly, to Eqs. 2 and 3 instantaneously neutralized by means of carbon dioxide dissolved in the liquid phase. On the other hand, Figure 3 shows nitrite and ammonium ions concentration vs. time dependencies obtained in the slurry reactor over various catalysts in nonbuffered aqueous solutions; these runs were conducted by bubbling the reaction suspension with a H_2-N_2 gas mixture. It is evident from Figure 3a that at these experimental conditions lower nitrite disappearance rates were observed in the presence of alumina-supported Pd and Pd-Cu catalysts. In these cases, much higher quantities of ammonium ions were detected in the liquid phase (Figure 3b), which confirms that both reaction kinetics and selectivity are drastically influenced by the increase of pH value of the aqueous solution during the reaction course. One can tentatively suppose that due to the accumulation of hydroxide ions in the liquid phase, there is a certain amount of these species physically adsorbed on the surface of either Pd monometallic or Pd-Cu bimetallic catalyst particles, which is also suggested by other investigators (Johansen and Buchanan, 1957; Vorlop and Tacke, 1989). The metal loadings in the catalysts employed are relatively low and the metallic clusters are less than 50–70 Å in diameter, because x-ray analysis did not show the metallic phase. For example, EXAFS examination of the CAT-2 sample revealed that metallic clusters consist of about 20 Pd atoms in a tentative shape of an octahedron with a diameter of 5.6 Å (Pintar et al., 1998a). Hence, the charging mechanism of the catalytic solid is more likely to be controlled by the γ-Al_2O_3 support, and occurs as a result of proton binding/release, which is pH dependent. During the liquid-phase nitrite reduction carried out in nonbuffered aqueous solutions, the increase of pH value of the liquid phase results in negative charge development, which arises due to the deprotonation of catalyst surface ($MOH_2^+ \Leftrightarrow MOH + H^+$, $MOH \Leftrightarrow MO^- + H^+$). Consequently, it is believed that a buildup of negative charge on the particle surface results in lower nitrite disappearance rates due to the enhanced repulsion between residual nitrite ions and the catalyst. Contrary to the results illustrated in Figure 2a, it is interesting to point out that at the operating conditions listed in Figure 3, the Pd-Cu bimetallic catalyst (CAT-3) in comparison to the CAT-2 sample enables much higher nitrite disappearance rates. It is speculated that the presence of the copper metallic phase on the alumina support makes the charge of a catalyst-solution interface less negative.

To further demonstrate the importance of textural properties of Pd-Cu bimetallics on the reaction under consideration, some experiments were carried out in which a physical mixture consisting of Pd/γ-Al_2O_3 and metallic copper particles was used as a catalyst. In these cases, the Pd-Cu active sites were formed *in situ* by the collision of particles; however, previous experiments (Pintar and Kajiuchi, 1995) have confirmed that the observed kinetics were not influenced by the collision probability. Although the concentration of active sites for nitrite removal was rather low, the results depicted in Figure 3a show that in this case nitrite disappears much faster than in the presence of the CAT-3 sample. For example, nitrite disappeared completely within less than 3 min (the shortest period in which our measurement had been made). Furthermore, in the presence of a physical mixture in the aqueous phase, about 95 mol. % of the initial nitrite content was transformed to nitrogen, even at pH noncontrolled conditions (Figure 3b). In the described experiment, the reaction was limited to contact of outer surfaces of Pd/γ-Al_2O_3 and Cu particles. Correspondingly, these results represent a good example to illustrate to what extent the diffusion of ionic species in the interior of even very small and porous particles could influence either reaction kinetics or selectivity of the catalytic nitrite reduction. According to the results concern-

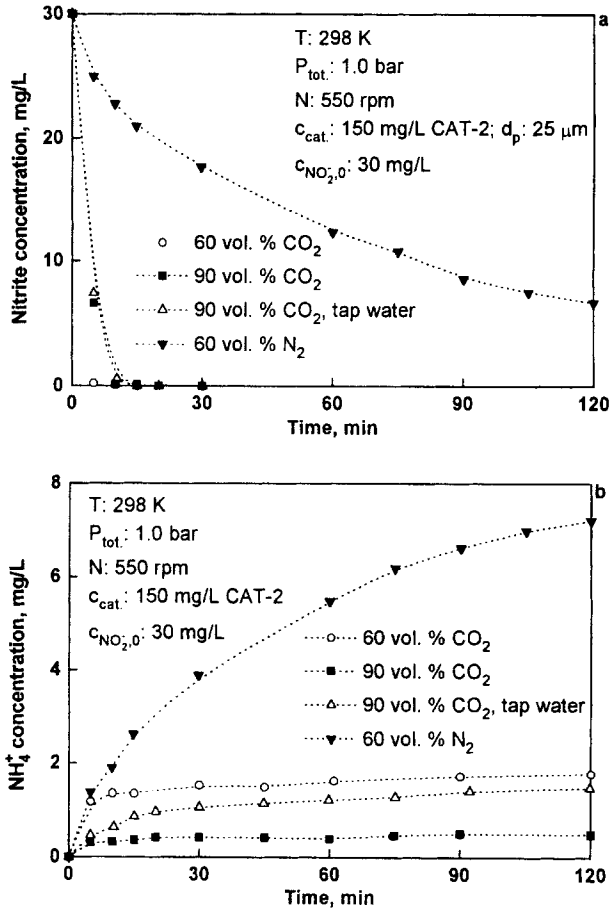

Figure 4. Nitrite (a) and ammonium (b) ions concentration as a function of time obtained in the slurry reactor using different reaction media and gas mixtures.

ing the reaction selectivity (Figures 2b and 3b), it is concluded that the liquid-phase hydrogenation of aqueous nitrite solutions can be efficiently carried out at pH-controlled conditions in the presence of the Pd(1 wt. %)/γ-Al_2O_3 catalyst. In order to achieve high nitrogen production yield, Pd-Cu bimetallic solids known as catalysts, which effectively promote liquid-phase nitrate reduction, should be employed only for the transformation of nitrates to nitrites. Furthermore, a comparison of data represented in Figures 2b and 3b with those obtained by Strukul et al. (1996), who also studied liquid-phase nitrite reduction in the presence of Pd monometallic and Pd-Cu bimetallic catalysts prepared by a sol-gel procedure, confirms that the use of solids synthesized by using the multistep wet-impregnation technique leads to lower production of ammonium ions.

Liquid-phase reduction experiments were also conducted in order to find out the effects of gas- and liquid-phase compositions on the catalytic nitrite hydrogenation. The results are illustrated in Figure 4; in the runs represented, the hydrogen partial pressure was equal to 0.1 and 0.4 bar, respectively. It can be seen in Figure 4a that the nitrite ion disappears very fast when carbon dioxide is employed as a hydrogen diluting agent. This is attributed to the low pH value of the aqueous solution, which was kept constant at pH = 4.7 during the entire reaction course. When hydrogen partial pressure was equal to 0.4 bar, the nitrite ion was completely transformed within a few minutes. On the other hand, when a hydrogen-nitrogen gas mixture was used as a reducing agent, the nitrite disappearance rate was still high in the very first stage of the reaction. Simultaneously, the pH value of the aqueous solution changed abruptly due to the formation of hydroxide ions, which made the surface of catalyst particles negatively charged. As discussed above, due to repulsion forces nitrite disappearance ceased, which is in agreement with the observations of other authors (Vorlop and Tacke, 1989; Hörold et al., 1993a). It can be further seen from Figure 4a that at the used operating conditions, composition of the reaction medium has no impact on the nitrite disappearance rate. This experimental finding was expected, since with respect to the structure of the nitrite ion there is no species available in tap water which could competitively adsorb to the Pd active sites (Pintar et al., 1998b). It is furthermore reported by Pintar et al. (1998b) that the ionic strength of the reaction medium, and, hence, the spatial extension of the double layer, has no meaningful influence on the reaction course, which confirms that no reaction steps of nitrite reduction take place in the liquid phase. Figure 4b clearly shows that the formation of ammonium ions is increased by increasing the hydrogen partial pressure. It is concluded that ammonia production is favored at pH noncontrolled conditions, or when the nitrite reduction is carried out in tap water. In the latter case, the enhanced ammonia formation can be attributed to the high concentration (270 mg/L) of hydrogen carbonate ions in drinking water (Pintar et al., 1998b). At the end, investigations were conducted in order to determine the role of the nitrate ion present in the liquid phase in the course of catalytic nitrite reduction. It is well documented that Pd(5 wt. %)/γ-Al_2O_3 is a good catalyst that promotes nitrite reduction; however, it is completely inactive for the liquid-phase nitrate transformation to nitrogen (Vorlop and Tacke, 1989; Pintar and Kajiuchi, 1995; Batista et al., 1997). In these runs, the initial nitrite concentration was equal to 74 mg/L and the hydrogen partial pressure was set to 0.4 bar; all other operating parameters were equal to those listed in the caption of Figure 4. It can be seen in Figure 5 that when only $NaNO_2$ was present in the aqueous solution at the beginning of the reduction run, at the given experimental conditions, 4.1 mg/L of ammonium ions were found in the liquid phase after the transformation of nitrites was completed. However, in the presence of nitrite as well as nitrate ions (100 mg/L) in the aqueous phase, the formation of ammonium ions was appreciably enhanced; at the end of the reaction, 10.5 mg/L of ammonium ions were detected in the aqueous solution. In the light of this experimental finding, it can be concluded that the nitrate ion, analogously to the hydrogen carbonate anion, reduces selectivity of the concerned reaction. On the other hand, chlorides and sulfates present in the liquid phase exhibit no influence on ammonia production (Pintar et al., 1998b). Therefore, it is believed that in the process of catalytic liquid-phase hydrogenation of aqueous nitrite solutions, anions with planar structure (that is, nitrates and hydrogen carbonates) hinder the desorption of gaseous intermediate and final products from the surface of supported Pd monometallic and Pd-Cu bimetallic catalysts.

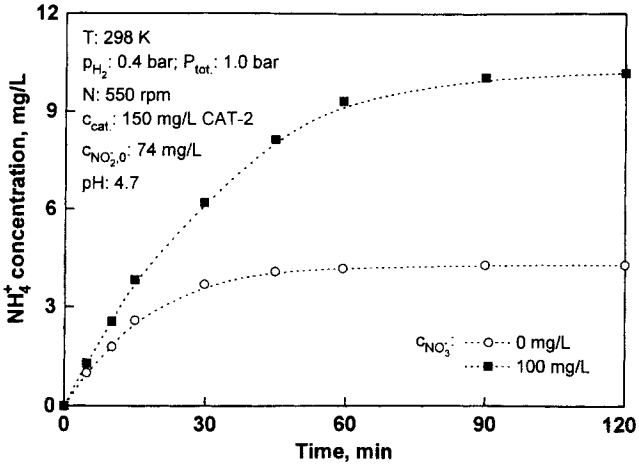

Figure 5. Influence of nitrates on the formation of ammonium ions in the course of catalytic liquid-phase nitrite reduction.

Figure 6 illustrates concentration of ammonium ions as a function of nitrite conversion obtained in the slurry reactor which was operated in a wide range of operating conditions (Table 2). It is evident that in any of the performed runs, the measured concentrations of ammonium ions are far below the maximum allowable concentration for drinking water. The reaction selectivity was found to be as high as 99 mol. %, which indisputably confirms that CAT-1 is suitable for the treatment of drinking water streams containing nitrites in appreciable quantities. Furthermore, the formation of hydroxylamine was not observed in any of the runs (detection limit of the applied spectrophotometric determination with *p*-nitrobenzaldehyde was equal to 0.01 mg/L NH_2OH). Consequently, a detailed study of the kinetics of liquid-phase nitrite reduction with hydrogen was carried out by using the Pd(1 wt. %)/γ-Al_2O_3 catalyst. Figure 7a shows the nitrite concentration as a function of time at different reaction temperatures with constant hydrogen partial pressure. Figure 7b presents the same dependence at various hydrogen partial pressures but at a constant reaction temperature. The experimental data points plotted in Figures 7c and 7d illustrate the nitrite concentration vs. time dependencies obtained in the slurry reactor at different catalyst loadings, as well as initial nitrite concentrations. These data demonstrate that the nitrite is irreversibly transformed to intermediate and final products at the reaction times, which make this denitrification technique attractive for large-scale operation. In Figure 8 nitrite disappearance rates are plotted as a function of instantaneous nitrite concentration in the reaction suspension. These rates were obtained by differentiating the data from Figures 7c and 7d. It can be seen in Figure 8a that the nitrite disappearance rate per unit weight of catalyst is independent of initial nitrite concentration provided that this concentration is less than or equal to 10 mg/L. However, at higher values of initial nitrite concentration, the measured reaction rates decrease, which implies that the kinetics of the investigated reaction is rather complex. The same phenomenon is depicted also in Figure 8b; the nitrite disappearance rate decreases by increasing the initial nitrite to catalyst concentration ratio. These findings might be ascribed to the catalyst deactivation, which already occurs to a substantial extent in the early stage of the hydrogenation run. Although the catalytic nitrite reduction was performed at a pH value below the isoelectric point of CAT-1 (that is, the catalyst surface was positively charged at actual operating conditions) and CO_2 was employed in order to eliminate the influence of produced OH^- ions on the reaction course, it seems that at the given operating conditions a certain amount of hydroxide ions is preferentially neutralized by protons adsorbed on the catalyst surface. The surface charge would in turn become less positive, which would (due to the coulombic repulsion)

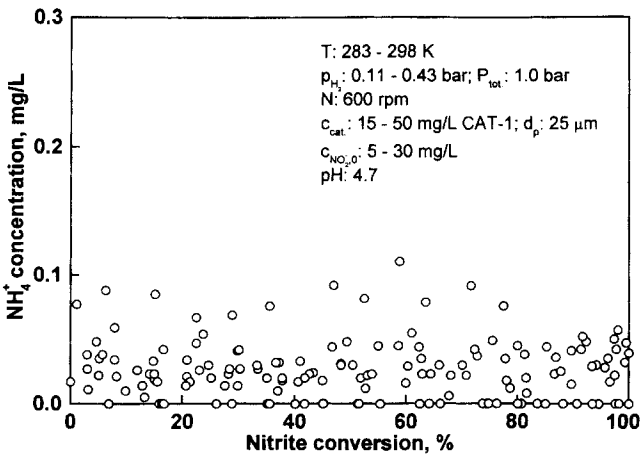

Figure 6. Concentration of ammonium ions as a function of nitrite conversion over the CAT-1 sample at various reaction conditions.

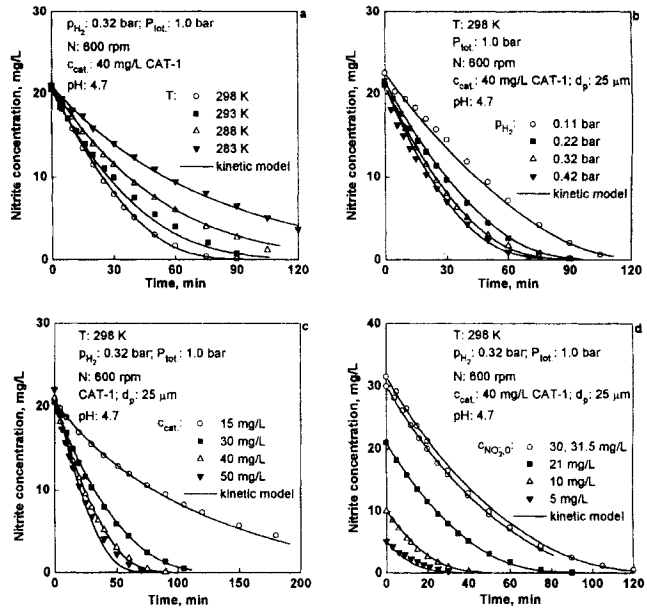

Figure 7. Nitrite concentration vs. time curves obtained in the slurry reactor in the course of liquid-phase nitrite reduction.

(a) Various reaction temperatures; (b) hydrogen partial pressures; (c) catalyst loadings; and (d) initial nitrite concentrations.

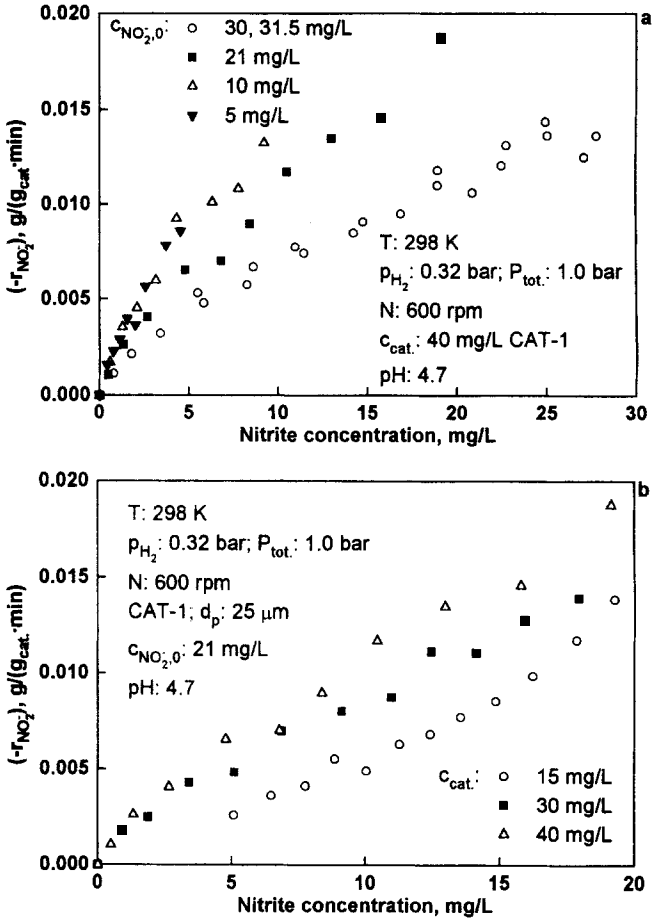

Figure 8. Nitrite disappearance rate as a function of instantaneous nitrite concentration in the slurry reactor at different initial pollutant concentrations (a) and catalyst loadings (b).

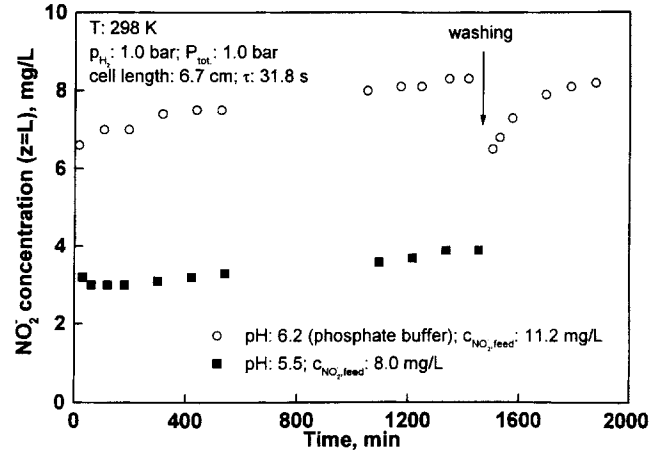

Figure 9. Catalyst activity tests of liquid-phase nitrite reduction carried out in a monolith reactor.

adversely affect the nitrite disappearance rate. This hypothesis was checked by carrying out catalytic liquid-phase nitrite reduction in a continuous-flow monolith reactor operating in the Taylor flow regime. The apparatus, the procedure for these measurements, and the reaction conditions are described in detail elsewhere (Berčič et al., 1997). The effluent nitrite concentrations as a function of onstream time are depicted in Figure 9. It can be seen on the basis of represented dependencies that the activity of the Pd metallic phase for destructive nitrite reduction slowly decreases. Nevertheless, it has been found that the activity of the Pd catalyst could easily be replenished by washing the reactor surface with a diluted HCl solution ($5 \cdot 10^{-4}$ mol/L in this case). It is therefore believed that the above described drop of CAT-1 activity in the process of liquid-phase nitrite hydrogenation could be attributed to the catalyst surface deprotonation, which is in agreement with the observation of other investigators (Oppenheim et al., 1967).

Reaction kinetics

In order to derive an intrinsic rate equation of the catalytic liquid-phase hydrogenation of aqueous nitrite solutions, simultaneous deactivation of the Pd(1 wt. %)/γ-Al_2O_3 catalyst was involved in calculations by considering the concentration of hydroxide ions in the Helmholtz layer. The intrinsic rate of nitrite disappearance in the presence of catalyst deactivation $(-r)_d$ is defined as (Froment and Bischoff, 1990)

$$(-r)_d = (-r)_0 \cdot f(d) \tag{4}$$

where $(-r)_0$ is the reaction rate without any catalyst deactivation, and $f(d)$ is the activity function which represents a slowdown correction to the reduction reaction because of the depletion of catalyst active sites by surface deprotonation. This activity function depends on the reaction conditions and catalyst properties; based on the discussion below, it is expected that the exponential function will best describe our results.

In the Helmholtz layer, electrostatic potential Φ (V) changes linearly with the distance from the catalyst particle surface, as follows

$$\Phi(x) = \Phi_s \cdot \left(1 - \frac{x}{a}\right) + \Phi_a \cdot \frac{x}{a} \tag{5}$$

According to the Gouy-Chapman-Stern model (Greef et al., 1985) for diluted and symmetrical electrolytes, the potential in the diffuse layer, which is the region between the bulk and the outer Helmholtz plane, varies exponentially with the distance from the catalyst surface

$$\Phi(x) = \Phi_a \cdot \exp^{-(x-a)/x_A} \tag{6}$$

Since liquid-phase nitrite hydrogenation represents a typical heterogeneously catalyzed irreversible reaction, and composition of the liquid phase (and consequently of the diffuse layer) has no influence on the nitrite disappearance rate, it is obvious that the use of only Eq. 5 is sufficient to describe quantitatively the effect of the electrostatic potential in the very vicinity of the catalyst surface on reaction kinetics. One should also note that, due to the neutralization of desorbed hydroxide ions by means of dissolved carbon dioxide, the electro-

static potential in the diffuse layer was equal to the one in the bulk liquid phase.

Decrease of Φ_s and Φ_a potentials in Eq. 5 is linearly proportional to the amount of surface protons being consumed by hydroxide ions produced and, correspondingly, to the instantaneous conversion of nitrites. When describing processes that take place at the solid–liquid interface (electrical double layer), the Maxwell-Boltzmann statistics are generally assumed to relate the concentration of ions at a specified position in the interface to its bulk concentration, and the electrostatic potential, thus

$$c(x,t) = c(\infty,t) \cdot \exp^{-[z \cdot F \cdot \Phi(x,t)]/R \cdot T} \tag{7}$$

Since z for the hydroxide ion is equal to -1, it results from Eq. 7 that the variation of the catalyst properties, that is, the decrease of the electrostatic potential in the inner layer, exponentially reduces the accessibility of nitrite ions to the outer Helmholtz plane. In other words, due to the enhanced repulsion forces between deprotonated catalyst surface and residual NO_2^- ions in the liquid phase, total concentration of active sites for subsequent catalytic cycles apparently decreases with reaction time. Deactivation of the Pd(1 wt. %)/γ-Al_2O_3 catalyst, which occurs in the course of liquid-phase hydrogenation of aqueous nitrite solutions, will be considered in the integral analysis of kinetic data by multiplying various reaction rate equations, typical of heterogeneous processes, by an appropriate decay term.

The intrinsic rate equation for the catalytic liquid-phase hydrogenation of aqueous nitrite solutions over the CAT-1 sample was developed by analyzing data of kinetic measurements, carried out in an isothermal slurry reactor at different initial nitrite concentrations, catalyst loadings, hydrogen partial pressures, and reaction temperatures. Seventeen data sets were collected in these hydrogenation experiments and analyzed by means of the integral analysis. Different rate equations derived on the basis of Langmuir-Hinshelwood, Eley-Rideal, and steady-state adsorption kinetic formulations (Table 3) were employed as a sink term in the respective mass balance equation describing the gradientless semi-batch CSTR reactor. For nitrite ions, the mass balance can be written as

$$\frac{dc}{dt} = (-r_{NO_2^-})_d \cdot \frac{m_{cat.}}{V_{reactor}} \tag{8}$$

$$\text{I.C.:} \quad t = 0; \quad c_{NO_2^-} = c_{NO_2^-,0}$$

$$t \geq 0; \quad c_{H_2} = \text{const.}, \quad T = \text{const.}$$

During preliminary experiments, the operating conditions were analyzed and adjusted in such a way that the reactor was operated in the kinetic regime. In subsequent calculations, the value of the effectiveness factor η was set to be equal to 1, since it had been found previously that at the given reaction conditions the nitrite disappearance rate is not influenced by pore or surface diffusion processes (Pintar et

Table 3. Tested Reaction Rate Equations

Eq.		Eq.	
I	$(-r) = \frac{k_1 \cdot C_{NO_2^-} \cdot C_{H_2}^{1/2}}{(1 + K_{NO_2^-} \cdot C_{NO_2^-} + K_{H_2} \cdot C_{H_2}^{1/2})}$	XI	$(-r) = \frac{k_1 \cdot C_{NO_2^-}^2 \cdot C_{H_2}^{1/2}}{(1 + K_{NO_2^-} \cdot C_{NO_2^-}^2) \cdot (1 + K_{H_2} \cdot C_{H_2}^{1/2})}$
II	$(-r) = \frac{k_1 \cdot C_{NO_2^-} \cdot C_{H_2}^{1/2}}{(1 + K_{NO_2^-} \cdot C_{NO_2^-} + K_{H_2} \cdot C_{H_2}^{1/2})^{1/2}}$	XII	$(-r) = k_1 \cdot C_{NO_2^-}^{n_1} \cdot C_{H_2}^{n_2}$
III	$(-r) = \frac{k_1 \cdot C_{NO_2^-} \cdot C_{H_2}^{1/2}}{(1 + K_{NO_2^-} \cdot C_{NO_2^-} + K_{H_2} \cdot C_{H_2}^{1/2})^2}$	XIII	$(-r) = \frac{k_1 \cdot C_{NO_2^-} \cdot C_{H_2}^{1/2}}{(1 + K_{NO_2^-} \cdot C_{NO_2^-})^{1/2} \cdot (1 + K_{H_2} \cdot C_{H_2}^{1/2})}$
IV	$(-r) = \frac{k_1 \cdot C_{NO_2^-} \cdot C_{H_2}^{1/2}}{(1 + K_{NO_2^-} \cdot C_{NO_2^-} + K_{H_2} \cdot C_{H_2}^{1/2})^3}$	XIV	$(-r) = \frac{k_1 \cdot C_{NO_2^-} \cdot C_{H_2}^{1/2}}{(1 + K_{NO_2^-} \cdot C_{NO_2^-})^2 \cdot (1 + K_{H_2} \cdot C_{H_2}^{1/2})}$
V	$(-r) = \frac{k_1 \cdot k_2 \cdot C_{NO_2^-} \cdot C_{H_2}^{1/2}}{k_1 \cdot C_{NO_2^-} + k_2 \cdot C_{H_2}^{1/2}}$	XV	$(-r) = \frac{k_1 \cdot C_{NO_2^-}^{1/2} \cdot C_{H_2}^{1/2}}{(1 + K_{H_2} \cdot C_{H_2}^{1/2})}$
VI	$(-r) = \frac{k_1 \cdot C_{NO_2^-}^{1/2} \cdot C_{H_2}^{1/2}}{(1 + K_{NO_2^-} \cdot C_{NO_2^-}^{1/2} + K_{H_2} \cdot C_{H_2}^{1/2})}$	XVI	$(-r) = \frac{k_1 \cdot C_{NO_2^-}^{1/2} \cdot C_{H_2}^{1/2}}{(1 + K_{H_2} \cdot C_{H_2}^{1/2})^{1/2}}$
VII	$(-r) = \frac{k_1 \cdot C_{NO_2^-}^{1/2} \cdot C_{H_2}^{1/2}}{(1 + K_{NO_2^-} \cdot C_{NO_2^-}^{1/2} + K_{H_2} \cdot C_{H_2}^{1/2})^{1/2}}$	XVII	$(-r) = \frac{k_1 \cdot C_{NO_2^-}^{1/2} \cdot C_{H_2}^{1/2}}{(1 + K_{H_2} \cdot C_{H_2}^{1/2})^2}$
VIII	$(-r) = \frac{k_1 \cdot C_{NO_2^-}^{1/2} \cdot C_{H_2}^{1/2}}{(1 + K_{NO_2^-} \cdot C_{NO_2^-}^{1/2} + K_{H_2} \cdot C_{H_2}^{1/2})^2}$	XVIII	$(-r) = \frac{k_1 \cdot C_{NO_2^-} \cdot C_{H_2}^{1/2}}{(1 + K_{NO_2^-} \cdot C_{NO_2^-})}$
IX	$(-r) = \frac{k_1 \cdot C_{NO_2^-} \cdot C_{H_2}^{1/2}}{(1 + K_{NO_2^-} \cdot C_{NO_2^-}) \cdot (1 + K_{H_2} \cdot C_{H_2}^{1/2})}$	XIX	$(-r) = \frac{k_1 \cdot C_{NO_2^-} \cdot C_{H_2}^{1/2}}{(1 + K_{NO_2^-} \cdot C_{NO_2^-})^{1/2}}$
X	$(-r) = \frac{k_1 \cdot C_{NO_2^-}^{1/2} \cdot C_{H_2}^{1/2}}{(1 + K_{NO_2^-} \cdot C_{NO_2^-}^{1/2}) \cdot (1 + K_{H_2} \cdot C_{H_2}^{1/2})}$	XX	$(-r) = \frac{k_1 \cdot C_{NO_2^-} \cdot C_{H_2}^{1/2}}{(1 + K_{NO_2^-} \cdot C_{NO_2^-})^2}$

*$(-r)$ = Nitrite disappearance rate.

al., 1998b). Investigators who have studied hydrogen chemisorption on noble metals have found that molecular hydrogen adsorbs dissociatively on Pd surface atoms (Knor, 1983); consequently, in the rate equations listed in Table 3, the hydrogen reaction order was set equal to 1/2. The concentration of hydrogen dissolved in the aqueous solution was almost constant during the run and was dependent only on reaction temperature and hydrogen partial pressure. Concentration of hydrogen in the liquid phase was calculated by using a correlation proposed by Fogg and Gerrard (1990)

$$x_g = \exp(-125.939 + 5528.45/T + 16.8893 \ln(T)) \quad (9)$$

To convert the mole fraction of hydrogen into common concentration units, such as mg H_2/L, the former equation was multiplied by the hydrogen partial pressure, water molar density (dissolved moles of hydrogen were neglected), and hydrogen molecular weight. The resulting equation reads

$$c_{H_2} = y_i \cdot \frac{P_{tot.}}{P_{tot.} = 1 \text{ bar}} \cdot \frac{x_g}{1 - x_g} \cdot \rho_{H_2O} \cdot \frac{M_{H_2}}{M_{H_2O}} \cdot 1000 \quad (10)$$

In the fitting procedure, the constants appearing in the tested reaction-rate equations were taken as parameters and their values were calculated by means of nonlinear regression. The Marquardt's minimization technique (Duggleby, 1984) was coupled with the fifth-order Cash-Kerp Runge-Kutta integration algorithm (Press et al., 1992) in order to calculate the values of residuals within the parameter minimization loop of the Marquardt's algorithm. The proportionally weighted sum of squares was minimized and calculated as

$$S_R = \sum_{i=1}^{N} (c_{NO_2^-,exp.} - c_{NO_2^-,calc.})^2 \cdot W_i \quad (11)$$

where the weighted factor W_i was set proportional to $(1/c_{NO_2^-})^2_{exp}$. This weighting ensures that during the parameter optimization, all data sets as well as the measured concentrations contribute proportionally to the calculated sum of squares despite the nitrite concentrations used. Since the integral analysis was applied in this study, the initial concentrations at $t = 0$ were set equal to the experimental ones; consequently, the differences between the measured and predicted concentrations become more pronounced for the experimental points measured at longer reaction time. To analyze the usefulness of the employed reaction rate equations (Table 3) in predicting experimental concentration vs. time dependencies, the measured data sets were combined into three groups in order to separately test the influence of nitrite concentration, hydrogen partial pressure, and temperature on the reaction course; hence, the first group includes eight data sets measured at constant hydrogen partial pressure (0.323 bar) and at constant temperature (298.15 K); the second group contains data from the first group plus four additional data sets measured at different partial pressures of hydrogen; the third group of data includes five additional data sets obtained at different reaction temperatures, hydrogen partial pressures, and initial nitrite concentrations. In Table 4 the goodness of fit of the examined rate equations for different groups of data is shown by the values of the calculated sum of squares, and also by the number of measured points which scatter around the calculated values less than $\pm 20\%$.

It follows from the calculated sum of squares (SS) shown in Table 4 that, on the basis of data in group 1, we cannot distinguish between the proposed reaction rate expressions, since at least six rate equations give comparable results. The same conclusion is obtained when we compare either the number of points ($N^{\pm 20}$) which lie within the 20% error band, or the corresponding reduced sum of squares (RSS). However, when

Table 4. Results of Nonlinear Regression Analysis of Kinetic Data in the Process of Catalytic Liquid-Phase Nitrite Reduction Carried Out in a Slurry Reactor

Equation (see Table 3)	No Deactivation Considered			Catalyst Deactivation Considered								
	Data Group 1 (102 Points)			Data Group 1 (102 Points)			Data Group 2 (138 Points)			Data Group 3 (198 Points)		
	SS	$N^{\pm 20}$	RSS	SS	$N^{\pm 20}$	RSS	SS	$N^{\pm 20}$	RSS	SS	$N^{\pm 20}$	RSS
I	11.3	68	0.53	2.8	84	0.23	6.3	118	0.37	7.14	174	0.655
II	22.6	53	0.38	4.94	76	0.76	14.9	86	0.60			
III	9.9	61	0.59	3.18	83	0.38	5.6	109	0.43			
IV	10.1	62	0.62	3.53	81	0.47	5.87	107	0.52			
V	11.3	68	0.538	2.85	83	0.18	6.34	118	0.37	7.14	174	0.690
VI	30.4	69	0.406	6.2	82	0.33	14.9	104	0.58			
VII	32.1	71	0.509	6.11	81	0.32	35.3	99	0.41			
VIII	53.1	52	0.15	6.15	82	0.33	20.7	106	0.37			
IX	11.3	68	0.53	2.8	84	0.21	6.23	112	0.35	8.23	169	0.90
X	30.3	69	0.40	6.11	81	0.32	17.8	100	0.43			
XI	20.2	64	0.33	11.5	75	0.37	9.19	99	0.65			
XII	29.8	56	0.10	5.5	75	0.32	13.0	84	0.41			
XIII	20.6	60	0.18	4.3	83	0.81	9.35	98	0.48			
XIV	9.9	61	0.59	3.1	83	0.38	6.01	109	0.44			
XV	49.5*	94*	0.74*				16.8	99	0.51			
XVI	45.1*	95*	0.81*				17.2	106	0.67			
XVII	42.9*	94*	0.73*				14.2	96	0.77			
XVIII	18.7*	96*	0.50*				13.2	101	0.25			
XIX	50.6*	78*	0.30*				21.7	101	0.74			
XX	16.7*	92*	0.45*				12.1	103	0.50			

*Kinetic data from group 2 were used in calculations considering no catalyst deactivation.

the measured and predicted concentration-time dependencies are compared in detail, one can see that the predicted profiles do not coincide with the measured ones; the calculations have shown that discrepancies between the measured and calculated values increase with reaction time. This again indicates that the catalyst deactivates during the hydrogenation process. Different algebraic expressions for the exponent in the exponential decay term of Eq. 7 were tested, and the best agreement between the measured and calculated values was achieved when the catalyst deactivation was set proportional to the amount of hydroxide ions produced during the nitrite hydrogenation. The simultaneous deactivation of CAT-1 is accounted for by the following relation

$$(-r_{NO_2^-})_d = (-r_{NO_2^-}) \cdot \exp\left(-b \cdot \frac{c_{NO_2^-,0} - c_{NO_2^-}}{c_{cat.}}\right) \quad (12)$$

When all tested equations were multiplied by the deactivation term of Eq. 12, much better agreement was obtained and the previously observed discrepancies between the predicted and measured nitrite concentrations vanished. Now, almost all tested equations give reasonably good fit of data in group 1. Furthermore, the rate equations were used to fit data from group 2. It is obvious that only Eqs. I, V, and IX (in Table 3) could describe the experimentally evaluated concentration-time dependencies obtained at different hydrogen partial pressures. When these equations are tested over all collected data (group 3), Eqs. I and V provide better results than Eq. IX. The temperature dependency of reaction rate (k_1, k_2) constants and adsorption (K_i) constants was introduced in calculations by assuming Arrhenius and van't Hoff relations.

The fitted values of parameters in Eqs. I and V are summarized in Table 5. The calculated values of adsorption constants are unrealistic, which is due to global minimization. This means that number 1 in the adsorption term of the rate equation I could be neglected and the resulting equation transforms into a form similar to Eq. V. We can further observe that the *five*-parameter Eq. V gives the same results as the *seven*-parameter Eq. I. The resulting equations confirm that Eq. V, which represents the steady-state adsorption (SSA) model (Shelstad et al., 1960; Teichner, 1975), is more suitable for describing the catalytic liquid-phase nitrite hydrogenation than models based on LHHW kinetic formulations. The number of parameters in Eq. V was further reduced by accounting for the reaction stoichiometry and temperature dependency of the hydrogen adsorption rate. Since the stoichiometric ratio between formed OH^- ions and the reacted nitrite ions are equal to 1, the value of parameter b in Eq. 12 was fixed to 1. The fitted value of activation energy for the hydrogen adsorption step is almost four times smaller than the one for surface reaction. It is well known that the value of activation energy for hydrogen chemisorption on noble metals is close to zero (Knor, 1983); hence, one can reasonably suppose that the rate of hydrogen adsorption (that is, catalyst surface regeneration) is temperature independent, which is in agreement with the performed statistical calculations. In spite of the reduced number of parameters (3 instead of 5), the resulting equation fits the experimentally measured data very well (172 data points within $\pm 20\%$ error, RSS = 0.638). The final form of the proposed kinetic model for catalytic liquid-phase nitrite hydrogenation is written as

$$(-r_{NO_2^-})_d = \frac{2.918 \cdot 10^{12} \cdot \exp\left(-\frac{93948}{R \cdot T}\right) \cdot c_{NO_2^-} \cdot c_{H_2}^{1/2}}{1.283 \cdot 10^{14} \cdot \exp\left(-\frac{93948}{R \cdot T}\right) \cdot c_{NO_2^-} + 0.0227 \cdot c_{H_2}^{1/2}} \cdot \exp\left(-\frac{c_{NO_2^-,0} - c_{NO_2^-}}{c_{cat.}}\right) \quad (13)$$

This equation assumes that the rate of adsorption of hydrogen is of the same order of magnitude as the rate of nitrite reduction, which means that a steady-state concentration of hydrogen is established on the catalyst surface. For illustration, at identical reaction conditions the reaction rate of catalytic nitrate hydrogenation, as compared to the rate of liquid-phase nitrite reduction, is lower by more than one order of magnitude. Due to the slower surface reaction step, the rate of hydrogen adsorption in the former case is sufficiently high at equilibrium; consequently, the kinetics of the catalytic nitrate reduction is well described by a rate equation of the Langmuir-Hinshelwood type (Pintar et al., 1996).

By using Eq. 13, the predicted nitrite concentration vs. time dependencies for various reaction conditions are shown in Figure 7 by solid curves. It can be seen that good agreement between the measured and calculated values is achieved, thus indicating that the assumptions and the kinetic model developed are reasonable. In Figure 10, a comparison between the measured and predicted nitrite concentrations as a function of time is illustrated for four experiments composed of two consecutive nitrite hydrogenations. In each of the two consecutive runs, the same batch of CAT-1 catalyst and the same initial nitrite concentrations were used. It is obvious from the presented results that, in the case of consecutive nitrite reductions, the predictions based on the proposed rate equation are also in very good agreement with the experimental values. These findings confirm that the exponential deactivation term of Eq. 13 properly accounts for the decay of catalyst activity even when amounts of H^+ ions removed from the catalyst surface are higher than those found during the runs performed for the collection of kinetic data (Figure 7).

Catalyst stability

Finally, the chemical stability of the Pd monometallic and Pd-Cu bimetallic catalysts was tested. For this purpose, the

Table 5. Fitted Values of Kinetic Parameters for Eqs. I and V

Eq.	k_1	k_2	$K_{NO_2^-}$	K_{H_2}	b
1	$1.29 \cdot 10^6 \cdot e^{(-26180/RT)}$		$1.45 \cdot 10^{-5} \cdot e^{(49693/RT)}$	$1411 \cdot e^{(0.0078/RT)}$	1.097
5	$6.27 \cdot 10^{11} \cdot e^{(-80654/RT)}$	$96.9 \cdot e^{(-20667/RT)}$			1.084

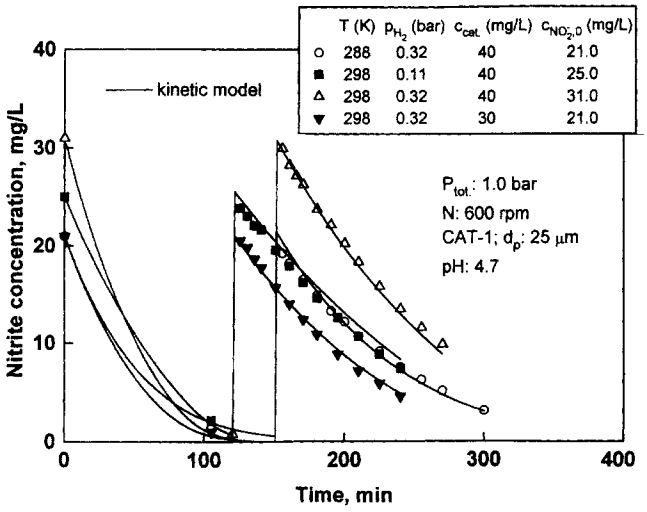

Figure 10. Nitrite concentration as a function of reaction time determined in the slurry reactor in consecutive runs using the same catalyst batch.

amounts of leached palladium and copper ions in aqueous-phase samples were determined by means of an ICP-AES method. In all samples, the concentrations of metal ions were found to be below the detection limits of both elements. Furthermore, the chemical analysis of fresh and used catalyst samples confirmed that no dissolution of active components took place during the above described experiments. Also, cold oxidation of Cu by ammonia leading to the appearance of Schweitzer's blue liquor was not observed. To elucidate the chemical resistance of the Pd-Cu catalyst, additional long-term stability tests were performed. The catalyst samples were exposed for one week to aqueous solutions of various pH values. For all pH values except pH = 2, the concentrations of Pd and Cu ions were found to be below the detection limit of the applied technique (Table 6). The high concentrations of Pd and Cu dissolved in the liquid phase at pH = 2 are associated with the instability of alumina support in aqueous solutions with a pH value below 3 (Ponec and Bond, 1995). Nevertheless, these experimental findings reflect high chemical stability of Pd monometallic and Pd-Cu bimetallic catalysts at neutral and slightly acidic conditions, which indicates that these solids can also be employed for direct drinking water purification. To conclude, the above results corroborate the fact that the catalyst deactivation observed in liquid-phase nitrite hydrogenation runs should be attributed to the release of protons from the catalyst surface due to their neutralization with produced hydroxide ions, which consequently leads to the buildup of negative charge on particles, rather than to modifications of chemical composition of employed solids in the course of liquid-phase nitrite reduction.

Table 6. Concentrations of Pd and Cu Ions, Leached from CAT-3 Sample at Different pH Values

pH, /	c_{Pd}, mg/L	c_{Cu}, mg/L
2.0	42	11.7
5.2	< 0.3	< 0.1
8.1	< 0.3	< 0.1
10.0	< 0.3	< 0.1

Conclusions

The results of this study demonstrate that the nitrite ion can be efficiently and selectively removed from contaminated groundwater by using alumina supported Pd catalysts. At pH = 4.7, the Pd(1 wt. %)/γ-Al_2O_3 catalyst converts more than 99% of initial nitrite content to nitrogen. Contrary to this, higher amounts of ammonium ions are observed over a Pd-Cu bimetallic solid, which might be attributed to inappropriate textural properties.

The intrinsic rate kinetic data over the Pd(1 wt. %)/γ-Al_2O_3 catalyst are well correlated by an extended *three*-parameter steady-state adsorption model of Hinshelwood, which accounts also for the simultaneous catalyst deactivation during the reaction course. Due to the partial neutralization of the produced hydroxide ions by means of carbon dioxide, the activity of the catalyst decreases exponentially with nitrite conversion, which is in agreement with the theory of electrical double layer. The activation energy of the surface reaction step was found to be 94 kJ/mol, while the surface reduction (regeneration) step is temperature independent at the given operating conditions. Good agreement between the measured and calculated concentration vs. time dependencies for single as well as consecutive reduction runs confirms that this model provides a valuable means of interpreting rate data concerning the catalytic liquid-phase hydrogenation of aqueous nitrite solutions.

Acknowledgments

Financial support from the Slovenian Ministry of Science and Technology under grant No. J2-0686 is gratefully acknowledged. The authors also thank the Nikki-Universal Co., Ltd. (Tokyo, Japan) for providing the alumina support used in the present study.

Notation

a = thickness of the Helmholtz layer, m
b = parameter in Eq. 12, dimensionless
c = concentration in liquid-phase, mg/L
$c(\infty)$ = bulk concentration, mg/L
$c_{cat.}$ = catalyst concentration in slurry reactor, mg/L
d_p = average catalyst particle diameter, μm
F = Faraday constant (96483 As/mol)
k_1 = reaction rate constant, L/($g_{cat.}$·min)
k_2 = hydrogen adsorption rate constant, (mg·L)$^{1/2}$/($g_{cat.}$·min)
K = adsorption constant, L/mg
$m_{cat.}$ = mass of catalyst in aqueous solution, g
M = molecular weight, g/mol
N = stirrer speed, rpm
p_{H_2} = hydrogen partial pressure, bar
$P_{tot.}$ = total operating pressure, bar
$(-r_{NO_2^-})$ = nitrite disappearance rate, mg/($g_{cat.}$·min)
R = gas constant, 8.3144 J/(mol·K)
t = reaction time, min
T = reaction temperature, K
$V_{reactor}$ = volume of reaction suspension, L
x = distance from catalyst surface, m
x_A = Debye length, m
x_g = mole fraction solubility, dimensionless
$X_{NO_2^-}$ = nitrite conversion, dimensionless
y_i = mole fraction of hydrogen in gas-phase, dimensionless
z = charge of ion, dimensionless
ρ = density, g/L

Subscripts

a = outer Helmholtz plane
d = deactivation
H_2 = hydrogen
H_2O = water
NO_2^- = nitrite ion
s = catalyst surface
0 = initial value

Literature Cited

Batista, J., A. Pintar, and M. Čeh, "Characterization of Supported Pd-Cu Bimetallic Catalysts by SEM, EDXS, AES and Catalytic Selectivity Measurements," *Catal. Lett.*, **43**, 79 (1997).

Berčič, G., A. Pintar, and J. Batista, "Catalytic Liquid-Phase Nitrite Reduction in a Monolith Reactor," *Proc. 1st European Congress on Chem. Eng.*, Florence, Vol. 1, p. 655 (May 4–7, 1997).

Canter, L. W., *Nitrates in Groundwater*, CRC Press, Boca Raton (1996).

Duggleby, R. G., "Analysis of Nonlinear Arrhenius Plots: An Empirical Model and a Computer Program," *Comput. Biol. Med.*, **14**, 447 (1984).

Fogg, P. G. T., and W. Gerrard, *Solubility of Gases in Liquids*, Wiley, Chichester (1990).

Froment, G. F., and K. B. Bischoff, *Chemical Reactor Analysis and Design*, 2nd ed., Wiley, New York (1990).

Greef, R., R. Peat, L. M. Peter, D. Pletcher, and J. Robinson, *Instrumental Methods in Electrochemistry*, Ellis Horwood, Chichester (1985).

Hörold, S., T. Tacke, and K. D. Vorlop, "Catalytical Removal of Nitrate and Nitrite from Drinking Water—I. Screening for Hydrogenation Catalysts and Influence of Reaction Conditions on Activity and Selectivity," *Environ. Tech.*, **14**, 931 (1993a).

Hörold, S., K. D. Vorlop, T. Tacke, and M. Sell, "Development of Catalysts for a Selective Nitrate and Nitrite Removal from Drinking Water," *Catal. Today*, **17**, 21 (1993b).

Johansen, P. G., and A. S. Buchanan, "An Electrokinetic Study by the Streaming Potential Method of Ion Exchange at Oxide Mineral Surfaces," *Aust. J. Chem.*, **10**, 392 (1957).

Johnson, D. P., "Spectrophotometric Determination of Oximes and Unsubstituted Hydroxylamine," *Anal. Chem.*, **40**(3), 647 (1968).

Kapoor, A., and T. Viraraghavan, "Nitrate Removal from Drinking Water—Review," *J. Environ. Eng.*, **123**(4), 371 (1997).

Knor, Z., "Chemisorption of Dihydrogen," *Catalysis—Science and Technology*, J. R. Anderson and M. Boudart, eds, Vol. 3, Akademie-Verlag, Berlin, p. 231 (1983).

Oppenheim, R. C., A. S. Buchanan, and T. W. Healy, "Surface Phenomena in the Photosynthesis of Hydrogen Peroxide by Aqueous Zinc Oxide Suspensions," *Aust. J. Chem.*, **20**, 1743 (1967).

Pintar, A., and T. Kajiuchi, "Catalytic Liquid-Phase Hydrogenation of Aqueous Nitrate Solutions," *Acta Chim. Slovenica*, **42**(4), 431 (1995).

Pintar, A., J. Batista, J. Levec, and T. Kajiuchi, "Kinetics of the Catalytic Liquid-Phase Hydrogenation of Aqueous Nitrate Solutions," *Appl. Catal. B: Environmental*, **11**, 81 (1996).

Pintar, A., J. Batista, I. Arčon, and A. Kodre, "EXAFS Study of γ-Al_2O_3 Supported Pd-Cu Bimetallic Catalysts," *HASYLAB Jahresbericht 1997*, Vol. 1, p. 689 (1998a).

Pintar, A., M. Šetinc, and J. Levec, "Hardness and Salt Effects on Catalytic Hydrogenation of Aqueous Nitrate Solutions," *J. Catal.*, **174**, 72 (1998b).

Ponec, V., and G. C. Bond, *Catalysis by Metals and Alloys*, Elsevier, Amsterdam (1995).

Press, H. W., S. A. Teukolsky, W. T. Vetterling, and B. P. Flannery, *Numerical Recipes—The Art of Scientific Computing*, 2nd ed., Cambridge University Press, Cambridge (1992).

Shelstad, K. A., J. Downie, and W. F. Graydon, "Kinetics of the Vapor-Phase Oxidation of Naphthalene over a Vanadium Catalyst," *Can. J. Chem. Eng.*, **38**, 102 (1960).

Skoda, F., M. P. Astier, G. M. Pajonk, and M. Primet, "Surface Characterization of Palladium-Copper Bimetallic Catalysts by FTIR Spectroscopy and Test Reactions," *Catal. Lett.*, **29**, 159 (1994).

Strohmeier, B. R., D. E. Leyden, R. S. Field, and D. M. Hercules, "Surface Spectroscopic Characterization of Cu/Al_2O_3 Catalysts," *J. Catal.*, **94**, 514 (1985).

Strukul, G., F. Pinna, M. Marella, L. Meregalli, and M. Tomaselli, "Sol-Gel Palladium Catalysts for Nitrate and Nitrite Removal from Drinking Water," *Catal. Today*, **27**, 209 (1996).

Tacke, T., and K. D. Vorlop, "Kinetische Charakterisierung von Katalysatoren zur selektiven Entfernung von Nitrat und Nitrit aus Wasser," *Chem. Ing. Tech.*, **65**(12), 1500 (1993).

Teichner, S. J., "Thermal and Photo-Interaction between Oxygen and Surfaces of Oxide Catalysts," *Proc. 3rd Int. Symp. on Heterogeneous Catalysis*, Varma, p. 56 (Oct. 13–16, 1975).

Vorlop, K. D., S. Hörold, and K. Pohlandt, "Optimierung von Trägerkatalysatoren zur selektiven Nitritentfernung aus Wasser," *Chem. Ing. Tech.*, **64**(1), 82 (1992).

Vorlop, K. D., and T. Tacke, "Erste Schritte auf dem Weg zur edelmetall-katalysierten Nitrat- und Nitrit-Entfernung aus Trinkwasser," *Chem. Ing. Tech.*, **61**(10), 836 (1989).

Manuscript received Mar. 31, 1998, and revision received July 20, 1998.